# Transient IR Absorption Study of Charge Carriers Photogenerated in Sulfur-doped TiO$_2$

Kan Takeshita[*]

Mitsubishi Chemical Group Science and Technology Research Center, Inc.,

1000, Kamoshida-cho, Aoba, Yokohama 227-8502, Japan


Akira Yamakata[†], Taka-aki Ishibashi[¶], Hiroshi Onishi[§]

Surface Chemistry Laboratory, Kanagawa Academy of Science and Technology (KAST),

KSP East 404, 3-2-1 Sakado, Takatsu, Kawasaki 213-0012, Japan


Kazumoto Nishijima and Teruhisa Ohno

Department of Material Science, Faculty of Engineering, Kyushu Institute of Technology,

1-1 Sensuicho, Tobata, Kitakyushu 804-8550, Japan


* Corresponding author.    E-mail address: 5503103@cc.m-kagaku.co.jp

Phone: +81-45-963-3155; Fax: +81-45-963-4261


Present address:

† Catalysis Research Center, Hokkaido University, Sapporo 001-0021, Japan

¶ Department of Chemistry, Graduate School of Science, Hiroshima University, Higashi-Hiroshima 739-8526, Japan

§ Department of Chemistry, Faculty of Science, Kobe University, Kobe 657-8501, Japan

**Abstract**

Sulfur-doped $TiO_2$ was prepared by two methods; one was simple oxidation annealing of $TiS_2$, the other was mixing of titanium isopropoxide and thiourea. These two sulfur-doped $TiO_2$ preparations showed fairly different photocatalytic activity under visible light. The dynamics of photogenerated charge carriers were studied by the transient absorption measurement in the region of mid-IR. In both samples, excitation by 532 nm pulse led to photocarrier generation to the same extent. Nevertheless, the reactivity of the photocarriers was totally different. Photogenerated electrons and holes transferred to reactant gas in the latter sample, whereas they did not in the former sample. We attributed the different carrier behavior to the difference in the distribution of S atoms or particle size. These observations can explain the difference in capability of photocatalysis under visible light.

# 1. Introduction

Semiconductor-based photocatalysis is a promising technology that has a variety of applications. The applications range from air purification by decomposition of harmful organic compounds to energy generation by photoinduced water splitting into $H_2$ and $O_2$.[1-3] Among many candidates, $TiO_2$ has proved to be the superior form of photocatalysis and has been widely utilized because of its high functionality, long-term stability and nontoxicity.[4] However, $TiO_2$ shows high reactivity only under ultraviolet light whose energy exceeds the band gap (3.2 eV for anatase crystalline phase). To make the best use of the solar spectrum, we need the development of photocatalysts that can yield high reactivity under visible light, and indeed, many researchers have tried to add visible light response to $TiO_2$.

One approach for acquiring a visible response is to introduce defects into the lattice through transition metals ion doping.[5-7] $TiO_2$ systems on which various photosensitizing dyes are adsorbed have also been widely investigated.[8-10] Recently, it has been reported that visible-light-response photocatalysts can also be produced by doping non-metal elements other than transition metals. For instance, nitrogen,[11] sulfur,[12] or carbon[13] doped $TiO_2$ were synthesized and they showed photocatalytic activity under visible light. Whether it is cationic or anionic, the doping of a foreign element into $TiO_2$ makes a donor or an acceptor level in the forbidden band and this level induces absorption of visible light. At the same time, however, this level may work as a carrier-recombination center, which decreases photocatalytic activity. Therefore, doping of a foreign element does not necessarily enhance response to visible light. To develop and improve visible-light-responsive photocatalysts, we should clarify what kind of doping or modification to $TiO_2$ is really effective in increasing activity under visible light.

Time-resolved infrared (TRIR) spectroscopy is a potential tool for this subject because it can give information of transient carriers in semiconductor photocatalysts. So far, several groups including us have applied this technique to reaction in oxidized semiconductors and related materials.[14-20] Electrons photoexcited in a semiconductor display structureless, monotonic absorption of IR light, which is attributed to transient absorption of electrons in conduction band or shallow midgap states.[18,19] The greatest advantage of employing IR light for probing is that the absorption signal from carrier electrons is not obstructed by other sources. Carrier electrons also give transient absorption in the visible region, but the bleach signal of catalysis itself or emission from excited catalysis falls on the target signal. For this reason, the IR region is more appropriate than the visible region for the

present purpose. Another advantage of our TRIR measurement system is that we can detect minute absorption changes in a long time scale. This enables us to evaluate even slight differences in photocatalytic activity of carriers through small absorbance changes.[18,19]

In the present study, we applied our TRIR system to sulfur-doped $TiO_2$ and investigated the dynamics of photogenerated charge carriers. We prepared sulfur-doped $TiO_2$ by two different methods. These two types of S-doped $TiO_2$ are interesting and are good models for examination because they have different forms of doping and fairly different photocatalytic activity under visible irradiation.[12,21,22] In the reference 12, S-doped $TiO_2$ was synthesized by oxidative annealing of $TiS_2$. The XPS measurement showed that S atoms were incorporated into the O site of $TiO_2$. On the other hand, in S-doped $TiO_2$ prepared by the method noted in references 21 and 22, S atoms substitute for some of the lattice Ti atoms. These studies indicate that forms of doping (e.g. oxidative number) are dependent on preparation conditions. Even more importantly, the difference of doping states has a strong influence on photocatalytic activity. Here we report the detailed dynamics of photogenerated holes and electrons in two types of S-doped $TiO_2$ and connect them with photocatalytic activity by use of a transient IR absorption study.


## 2. Experiment

In this study, we prepared sulfur-doped $TiO_2$ by two methods. In the first method, S-doped $TiO_2$ was synthesized by oxidation annealing of titanium disulfide ($TiS_2$) powder (High Purity Chemicals Laboratory Co., Ltd.) at 300 - 600 $^{o}$C. In the second method, S-doped $TiO_2$ was prepared by mixing titanium isopropoxide and thiourea in ethanol, subsequent evaporation and calcination (under air at 500 $^{o}$C). The details of each preparation procedure are shown in the literature.[12,21,22] After the preparation, S-doped $TiO_2$ powder was dispersed in water and spread on a $CaF_2$ plate. The density of the powder was 1 - 1.5 mg / $cm^2$.

Time resolved infrared absorption measurement was conducted using systems similar to those previously reported.[23,24] For an excitation pulse, we used the second (532 nm) or third (355 nm) harmonics of Q-switched Nd:YAG laser (10 ns pulse). The excitation pulse energy was 0.2 - 2 mJ / $cm^2$ and the repetition rate was 0.03 - 10 Hz. A probe light (emitted from the glober source) was focused on the sample plate with an ellipsoidal mirror. The transmitted light was dispersed in a monochromator of 50 cm focal length and the monochromatic output

was detected by an MCT (mercury-cadmium-telluride) detector. The MCT output was amplified in AC-coupled amplifiers and accumulated in a digital sampling oscilloscope as a function of delay time at a fixed wavelength. Temporal profiles were reconstructed to transient IR absorption spectra at different delay times. The time-resolution was about 50 ns, which was determined by the response of the detector. Time-resolved infrared absorption was measured at room temperature under vacuum or desired gas reactants.

The photocatalytic activity of S-doped $TiO_2$ was characterized in terms of the degradation of an organic dye, methylene blue. Briefly, 100 mg of each photocatalyst was suspended in 5 ml of methylene blue aqueous solution (50 mmol $dm^{-3}$). The solution was stirred in the absence of light to attain the equilibrium adsorption on the catalyst surface. The solution was then irradiated during stirring for 10 minutes using a 1000W Xe lamp. The short-wavelength components of the light were removed by cutoff glass filters. The extent of dye photodecomposition was estimated by measurement of the UV-VIS absorption spectrum.

## 3. Results
### 3-1. Characteristics and photocatalytic activity of S-doped $TiO_2$

When $TiS_2$ powder is calcined under air, sulfur atoms in $TiS_2$ are gradually replaced by oxygen atoms. In this process, we can control content of sulfur atoms by varying calcination temperature and time. Figure 1 shows the change of absorption spectrum of $TiS_2$ by calcination under air, at 300 $^o$C for 30 minutes, at 500 $^o$C for 30 minutes, or at 600 $^o$C for 2 hours. This spectrum suggests that most parts of $TiS_2$ powder remained unchanged at 300 $^o$C but that it was nearly completely transformed into $TiO_2$ at 600 $^o$C.

We refer to $TiS_2$ powder annealed at 500 $^o$C as the 'S-doped $TiO_2$ sample

A' hereafter.

We also prepared S-doped $TiO_2$ from titanium isopropoxide and thiourea. Some of the authors have previously reported the characteristics of this sample, such as UV-visible absorption and XPS spectrum.[21] In this work, we call this sample the 'S-doped $TiO_2$ sample B'. The atomic content of S atom in sample B has been reported as 0.5 -1.6 %.[21] In addition, we presume that the S atom content in sample A is roughly the same as sample B because both sample A and B absorb visible light to the same extent.

The photocatalytic activity of the S-doped $TiO_2$ samples A and B was evaluated by measuring the decomposition rates of methylene blue in aqueous solution. The results are shown in Figure 2. Both sample A and B showed strong activity under UV irradiation. However, response to visible light was considerably different between sample A and B. Sample A had only a little activity under visible irradiation, whereas sample B showed fairly large activity.

Figure 3 presents SEM images of sample A and B. A particle of sample A had a diameter of 1-2 μm, which was derived from the start material - $TiS_2$ powder.

It is known that the particle size of $TiO_2$ synthesized from titanium isopropoxide is tens of nanometers.[8] Presumably, S-doped $TiO_2$ sample B has a similar particle size.

**3-2. Transient absorption spectra and decay**

Figure 4A depicts transient absorption spectra of S-doped $TiO_2$ sample A in the mid-IR region when it was excited by ultraviolet (355 nm) or visible (532 nm) pulse. These spectra were measured in the atmosphere. In both excitation wavelengths, we observed broad unstructured transient absorption spectra that monotonously increased in intensity with decreasing wavenumber. This absorption is attributed to the intra-band transition of free electrons in the conduction band and optical transitions of trapped electrons from shallow midgap states to the conduction band.[18] Although the relative intensity of the transient absorption was considerably different between 355 nm and 532 nm excitation, the shape of the spectrum was almost identical. These observations show that free charge carrier generation occurred not only by 355 nm light excitation but also by 532 nm light excitation. However, the quantity of charge carrier generation was much larger by 355 nm light than by

532 nm light.

The transient absorption spectra for S-doped $TiO_2$ sample B are shown in figure 4B. Again, the excitation wavelength was 355 or 532 nm. We observed the same broad unstructured transient absorption as we observed in sample A. The difference in the shape and intensity of the spectra by the excitation wavelength was nearly the same as that observed in sample A.

The decay measurement and analysis of the transient absorption under various gas reactants is helpful in investigating the kinetics of photogenerated carriers in these samples.[19] Figures 5A and 5B show the decay of transient absorption at 2000 cm$^{-1}$ after 355 nm pulse excitation for S-doped $TiO_2$ samples A and B, respectively. The measurements were conducted in the presence of 10 Torr oxygen, water vapor, or methanol vapor. Measurements under vacuum conditions were also conducted for reference. In sample A, the decay was accelerated by the presence of oxygen, whereas it was decelerated by water vapor. Electrons are consumed by recombination with holes and also by reactions with adsorbates.[19,20] Therefore, the oxygen-induced quench is ascribed to the reaction of electrons with adsorbed oxygen. On the other hand, the deceleration of decay by water vapor can be explained by the quenching of the hole. Holes photogenerated in the valence band of $TiO_2$ oxidize water to oxygen.[2,4] In this experimental condition, it is considered that hydroxyl anions effectively capture the holes in the initial step of the oxidation.

Although these acceleration and deceleration behaviors were in good agreement with the result of the same experiments for $TiO_2$ or $Pt/TiO_2$[19] in sample A, the situation was somewhat different in sample B. Oxygen accelerated the signal decay as it did in sample A, but deceleration by water did not occur. This fact means that holes photogenerated in sample B did not have the ability to oxidize water. We also measured transient absorption under methanol vapor, because alcohol such as methanol is known as a strong scavenger of holes. The result is also shown in figure 5B. As expected, the decay was decelerated because of quenching of the holes by methanol vapor.

The results shown in figures 5A and 5B explain the activity of each photocatalyst under ultraviolet light. As a whole, both sample A and B had photocatalytic activity under UV light, although the activity of sample B was smaller than sample A. We next conducted the same experiment using 532 nm pulse light excitation to examine the activity under visible light. We present the results in Figures 6A and 6B. The decay features were considerably different between ultraviolet and visible excitation. First of all, in sample A, the decay was hardly affected by gas reactants. This result indicates that electrons and holes generated by visible light excitation did not move to gas reactants. In sample B, the decay was accelerated by oxygen and decelerated by methanol, but the extent of rate changes was rather smaller than observed by ultraviolet excitation. This fact means that electrons and holes are less able to move to reactants by visible excitation than by UV excitation.

In terms of photocatalytic activity, the result shown in Figures 6A and 6B proved that sample A did not work as photocatalysis under 532 nm light, but that sample B worked even under 532 nm light. This is correlated to the photocatalytic feature shown in Figure 2, and a detailed interpretation will be given in the next section.

Figure 7 shows the initial intensity of the transient absorption of S-doped $TiO_2$ samples A, B and $TiS_2$ annealed at 600 $^{\mathrm{o}}$C. $TiS_2$ powder annealed at 600 $^{\mathrm{o}}$C gave only a tiny transient absorption with the irradiation of 532 nm light because it has almost no absorption at this wavelength. (The spectrum shown in figure 1 indicates that $TiS_2$ was almost completely transformed into $TiO_2$ at this temperature.) The initial intensities of transient absorption observed for samples A and B were nearly the same, and they were 10 times as large as that observed for $TiS_2$ annealed at 600 $^{\mathrm{o}}$C, regardless of 1 / 10 excitation pulse energy. Since the initial intensity of transient absorption reflects the quantity of photogenerated electrons, this result means that photocarrier generation in samples A or B was about 100 times as frequent as that in $TiS_2$ annealed at 600 $^{\mathrm{o}}$C. It is interesting that photo carrier generation occurred to the same extent in both samples A and B, but the mobility of the photocarriers was considerably

different.

## 4. Discussion

In this section, let us discuss the differences in photocatalytic activity between S-doped $TiO_2$ samples A and B. Photoexcitation of samples with light of an energy that matches the band gap yields electron-hole pairs. Photogenerated electrons and holes can migrate to the surface and react with adsorbed reactants, or they may undergo undesired recombination. The photocatalytic efficiency depends on the competition between these two processes, that is, the ratio of reaction to recombination. The ratio of reaction to recombination depends on the electronic properties of the photocatalyst (e.g. energy level of CB, VB and trap states). Therefore, to discuss the differences in photocatalytic efficiency, we first consider the electronic properties of S-doped $TiO_2$.

$TiO_2$ has a wide band gap of 3.2 eV in the anatase crystalline phase. The edge of the valence band is at 3.0 eV versus NHE. The conduction band minimum is located at - 0.2 eV versus NHE. Doping of the S atom perturbs CB or VB (or both of them), and produces states in the band gap of $TiO_2$ that absorb visible light (Figure 8). Umebayashi et al. analyzed the band structures of S-doped $TiO_2$ by *ab initio* calculation.[12,22] According to their calculation, an electron-occupied level appears slightly above the VB, which contributes to visible absorption. Such band formation is possible if the quantity of doped S atom is adequate. If the quantity of S atoms is very small and S doped sites are isolated in bulk $TiO_2$, the doped S atom works as a trap state, like a 'defect'. The different preparation methods between samples A and B might affect the form of band and trap formation.

We here propose the following presumption to explain the difference of photocatalytic activity; the distribution of S atoms is different between samples A and B (Figure 9). In sample A, S atoms exist mainly in the central part of particles. In sample B, on the other hand, the distribution of S atoms is rather uniform, which means S atoms also exist near the surface. These different distributions of S atoms are easily inferred from each preparation method. Sample A is synthesized by annealing of a $TiS_2$ particle. In the annealing process, firstly O atoms replace S atoms near the surface. Then this replacement gradually spreads to the inner part of the particle. Consequently, the core of the particle has a larger

content of S atoms than the surface. Meanwhile, S atoms derive from thiourea in sample B. Hence S atoms must exist near the surface to a certain extent. Although these assumptions are currently rather speculative, they can well explain the experimental results as shown below.

Before explaining photocatalytic reactions under UV and visible light, we here describe states in an S-doped $TiO_2$ particle as the following four distinctive sites:

(i) A site that can absorb 355 nm light (unperturbed $TiO_2$)

(ii) A site that can absorb 532 nm light (induced by doping of S atoms)

(iii) A trap site that can catch photogenerated holes (induced by doping of S atoms)

(iv) A reaction site

The distribution of these (i) - (iv) sites should be determined by the distribution of S atoms. Now we are ready to explain the different behavior of photogenerated carriers between samples A and B. The discussion is developed below.

Figure 5 shows the activity of the carriers under UV irradiation. Near the surface, a particle of sample A has almost the same structure as $TiO_2$. Most parts of UV light are absorbed in the proximity of the surface. Accordingly, the activity of photogenerated carriers is the same as those in pure $TiO_2$. Meanwhile, a particle of sample B has trap states (site iii) near the surface, so that the activity of carriers is different from carriers in pure $TiO_2$. UV light irradiation generates holes in the valence band and these holes are eventually captured by the trap states. Once the trap sites catch holes,

This difference in the reactivity of holes with water clearly appears in figures 5A and 5B. A large amount of energy is required to oxidize water because of the presence of an overpotential. The experimental results indicate that the holes photogenerated in sample B do not have enough energy to oxidize water or hydroxyl anion. However, they can oxidize methanol (Figure 5B) and methylene blue (Figure 2). Methanol strongly adsorbs on the photocatalyst surface as a methoxy species. This fact means that methanol can be oxidized through direct hole transfer from the photocatalyst without a hydroxyl radial.[20] In terms of the oxidation potential, the energy required for the oxidation of methanol is smaller than that required for the oxidation of water. Taking these facts into consideration, it is not strange that holes photogenerated in sample B, which do not have enough energy to oxidize water, can oxidize methanol. The oxidation of methylene blue can also be explained by the direct hole transfer. In addition, the experiment shown in figure 2 was conducted in the solution condition, where some species other than a hydroxyl radical may relate to oxidative decomposition.

Figure 6 shows the activity of the carriers under visible irradiation. In sample A, most of site (ii), which absorbs visible light, is located at the center of the particle. Therefore, with visible irradiation, free carriers are generated mainly in the core of the particle. These carriers disappear through a recombination process in the semiconductor particle before migrating to outside gas reactants. This means that the existence of gas reactants has almost no influence on the decay process of free electrons. This presumption is supported by the experimental results shown in figure 6A. On the other hand, in sample B, site (ii) is distributed also on the surface. Carriers generated by visible excitation in site (ii) can move to site (iv), where a gas reactant extracts a carrier from the photocatalyst.

Another possible reason for the difference in activity between samples A and B is the difference in particle size. The SEM images of samples A and B (Figure 3) showed that the diameter of the sample A particle was 1 to 2 $\mu$m and that the diameter of the sample B particle was far smaller than sample A (tens of nanometers). In sample A, electrons and holes generated in the core of the particle disappear through recombination before migrating to the surface, whereas, in sample B, they can reach the surface because of the short migration path length. This assumption can also explain the difference of photocatalytic efficiency under visible light, together with the difference in the distribution of S atoms as mentioned above.

**5. Summary**

We investigated the behavior of photogenerated charge carriers in two types of sulfur-doped TiO$_2$ (samples A and B) by transient absorption measurement in the region of mid-IR. The activity of photocarriers was fairly different between these two samples. In sample A, the behavior of the UV-light-generated electrons and holes was in good agreement with the result of the same experiments for pure TiO$_2$. On the other hand, in sample B, UV-light-generated holes did not have the ability to oxidize water, which is related to the existence of trap states near the surface. Excitation by 532 nm pulse led to photocarrier generation to the same extent in both samples. However, the reactivity of the photocarriers was totally different. Photogenerated electrons and holes migrated to reactant gas species in sample B, whereas they did not in sample A. We explained all these experimental results by

the difference in the distribution of S atoms or the particle size.

**References**

1. A. Fujishima, K. Honda, Nature 37 (1972) 238.

2. M.A. Fox, M.T. Dulay, Chem. Rev. 93 (1993) 341.

3. A. Heller, Acc. Chem. Res. 28 (1995) 503.

4. M.R. Hoffmann, S.T. Martin, W. Choi, D.W. Bahnemann, Chem. Rev. 95 (1995) 69.

5. A.K. Ghosh, H.P. Maruska, J. Electrochem. Soc. 124 (1977) 1516.

6. W. Choi, A. Termin, M.R. Hoffmann, J. Phys. Chem. 98 (1994) 13669.

7. M. Anpo, Catal. Surv. Jpn. 1 (1997) 169.

8. B. O'Regan, M. Grätzel, Nature 353 (1991) 737.

9. Y. Tachibana, J.E. Moser, M. Grätzel, D.R. Klug, J.R. Durrant, J. Phys. Chem. 100 (1996) 20056.

10. R. Abe, K. Hara, K. Sayama, K. Domen, H. Arakawa, J. Photochem. Photobiol. A Chem. 137 (2000) 63.

11. R. Asahi, T. Morikawa, T. Ohwaki, K. Aoki, Y. Taga, Science 293 (2001) 269.

12. T. Umebayashi, T. Yamaki, H.Itoh, K. Asai, Appl. Phys. Lett. 81 (2002) 454.

13. H. Irie, Y. Watanabe, K. Hashimoto, Chem. Lett. 32 (2003) 772.

14. T.A. Heimer, E.J. Heilweil, J. Phys. Chem. B 101 (1997) 10990.

15. H.N. Ghosh, J.B. Asbury, T. Lian, J. Phys. Chem. B 102 (1998) 6482.

16. H.N. Ghosh, J.B. Asbury, Y. Weng, T. Lian, J. Phys. Chem. B 102 (1998) 10208.

17. J.B. Asbury, E. Hao, Y. Weng, T. Lian, J. Phys. Chem. B 104 (2000) 11957.

18. A. Yamakata, T. Ishibashi, H. Onishi, Chem. Phys. Lett. 333 (2001) 271.

19. A. Yamakata, T. Ishibashi, H. Onishi, J. Phys. Chem. B 105 (2001) 7258.

20. A. Yamakata, T. Ishibashi, H. Onishi, J. Phys. Chem. B 107 (2003) 9820.

21. T. Ohno, T. Mitsui, M. Matsumura, Chem. Lett. 32 (2003) 364.

22. T. Ohno, M. Akiyoshi, T. Umebayashi, K. Asai, T. Mitsui, M. Matsumura, Appl. Catal. A 265 (2004) 115.

23. K. Iwata, H. Hamaguchi, Appl. Spectrosc. 44 (1990) 1431.

24. T. Yuzawa, C. Kato, M.W. George, H. Hamaguchi, Appl. Spectrosc. 48 (1994) 684.

**Figure captions**

Figure 1

Diffuse reflectance spectra of $TiS_2$ annealed at 300 $^o$C, at 500 $^o$C, or at 600 $^o$C, and unannealed $TiS_2$. Spectrum of S-doped $TiO_2$ sample B is also shown for the comparison.


Figure 2

Photocatalytic activity of the S-doped $TiO_2$ samples A and B, which was evaluated by decomposition rates of methylene blue. The horizontal axis represents 'cut-off wavelength' for irradiation of white light from a Xe lamp. (For example, '420 nm' means that wavelength shorter than 420 nm was cut.) Photocatalytic activity of the standard $TiO_2$ (ST-01, Ishihara Sangyo) and $TiS_2$ annealed at 600 $^o$C are also shown for the comparison.


Figure 3

SEM images of S-doped $TiO_2$ sample A and B.


Figure 4

Transient absorption spectra of S-doped $TiO_2$ samples A and B in the mid-IR region at 1 ms after pulse excitation.


Figure 5

Comparison of the decay of the transient absorption at 2000 cm$^{-1}$ under various gas reactants. Excitation wavelength was 355 nm. Figures 5A and 5B show the signals for sample A and B, respectively.


Figure 6

Comparison of the decay of the transient absorption at 2000 cm$^{-1}$ under various gas reactants. Excitation wavelength was 532 nm. Figures 6A and 6B show the signals for sample A and B, respectively.


Figure 7

Comparison of the initial intensity of the transient absorption among S-doped $TiO_2$ sample A, B and $TiS_2$ annealed at 600 $^o$C.

Figure 8

Estimated energy diagram of S-doped $TiO_2$.


Figure 9

Proposed difference in distribution of S atoms in S-doped $TiO_2$ samples A and B. (Dots represent doped S atoms.)

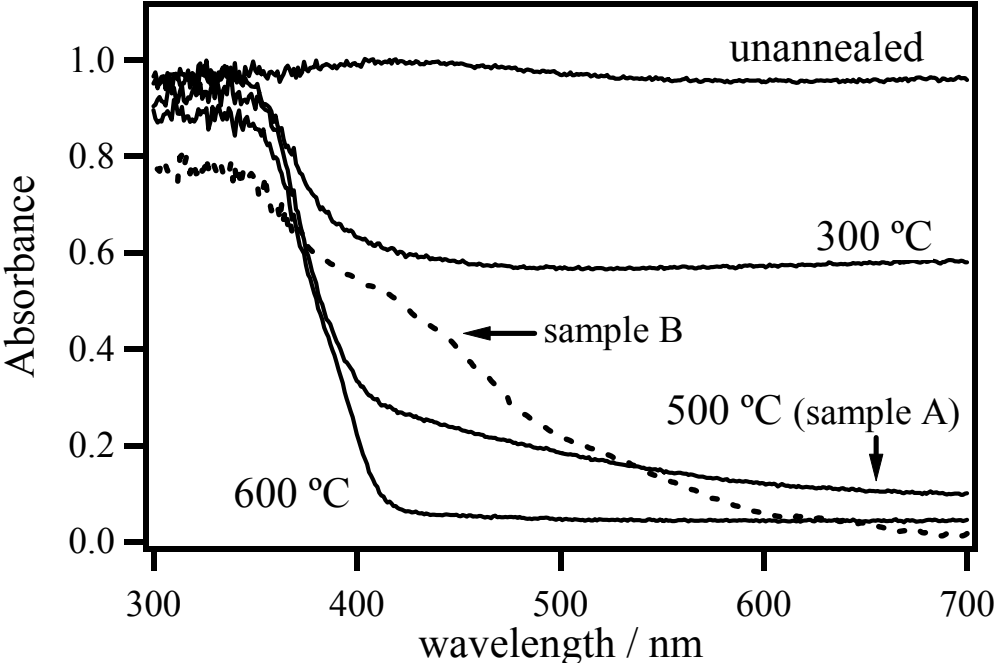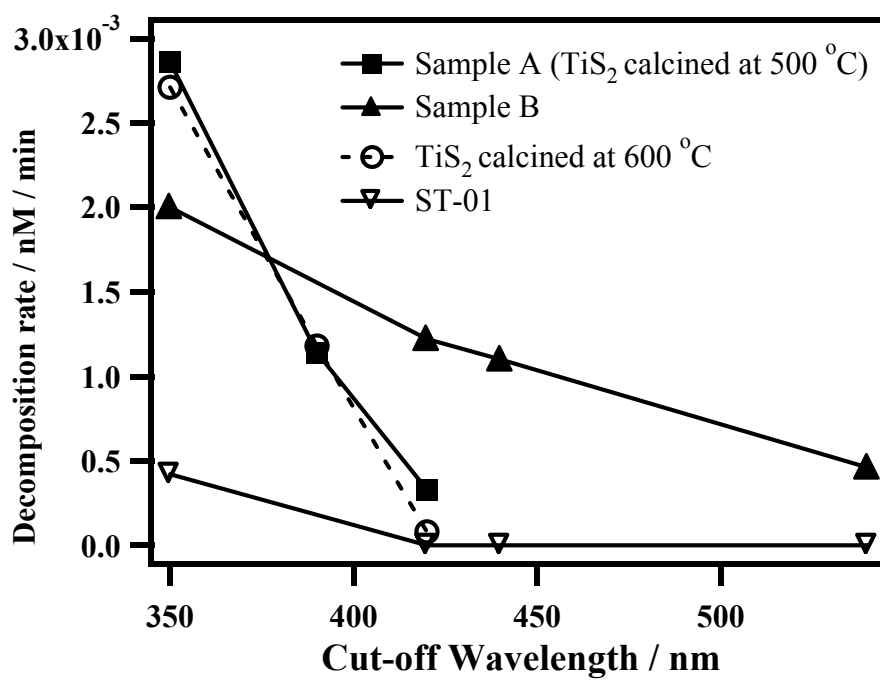**Figure 1**                                                                                                **Takeshita et al.**
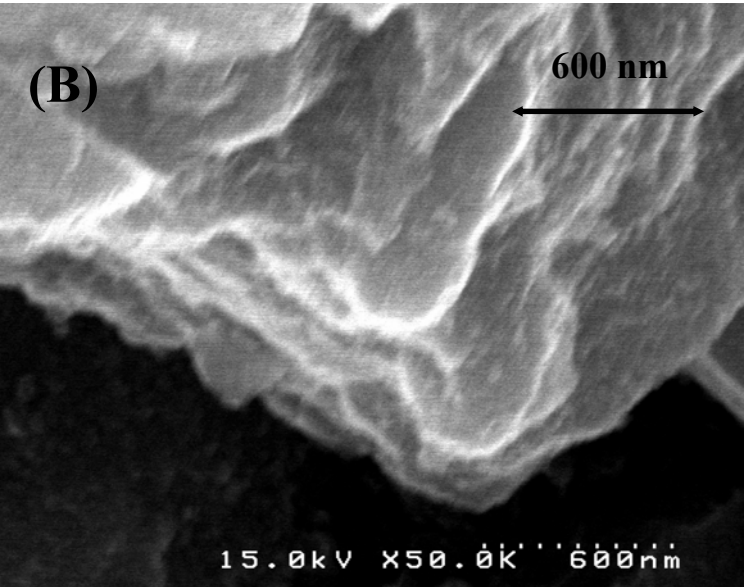
**Figure 2** Takeshita et al.

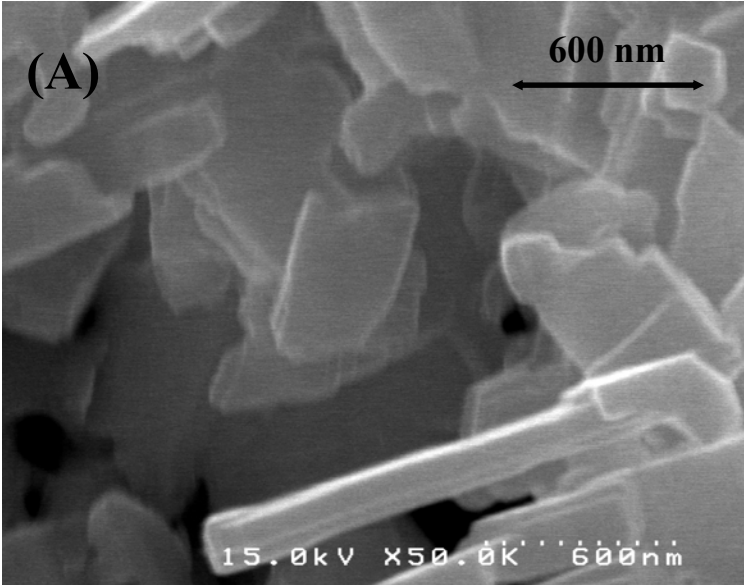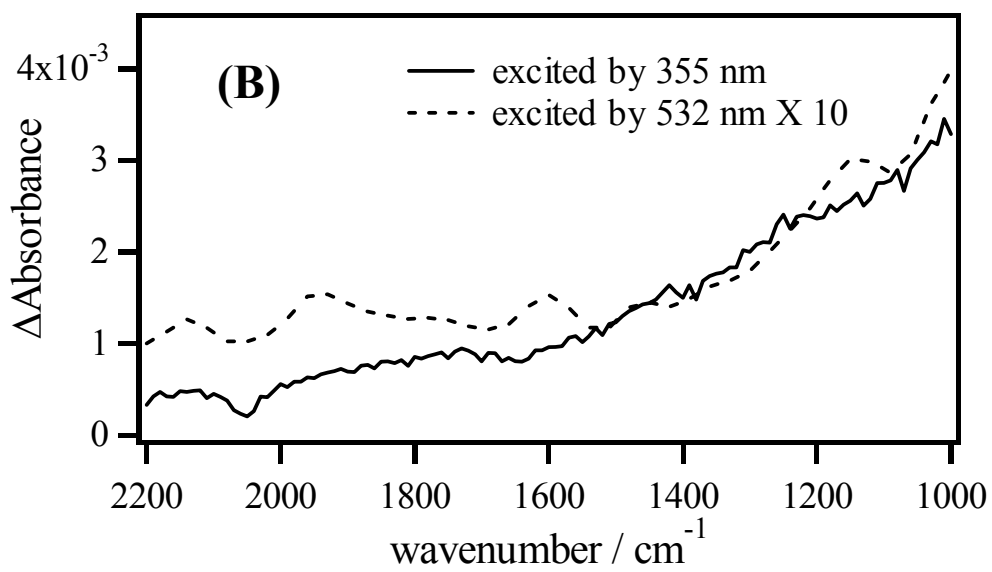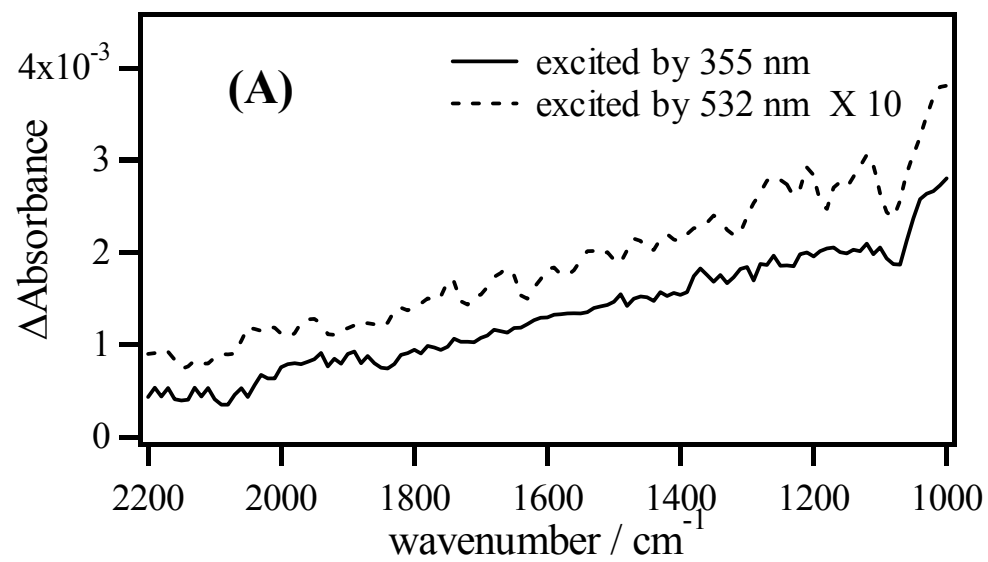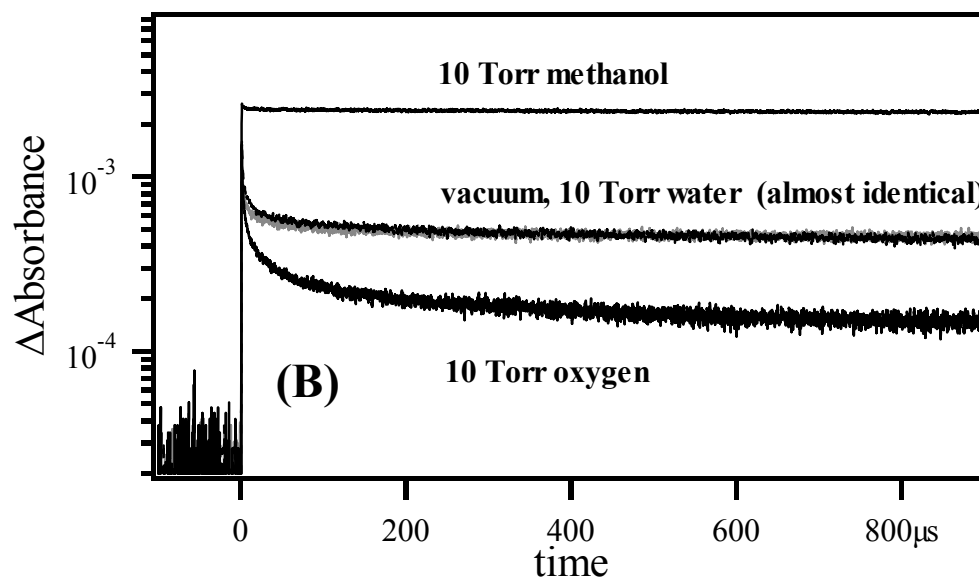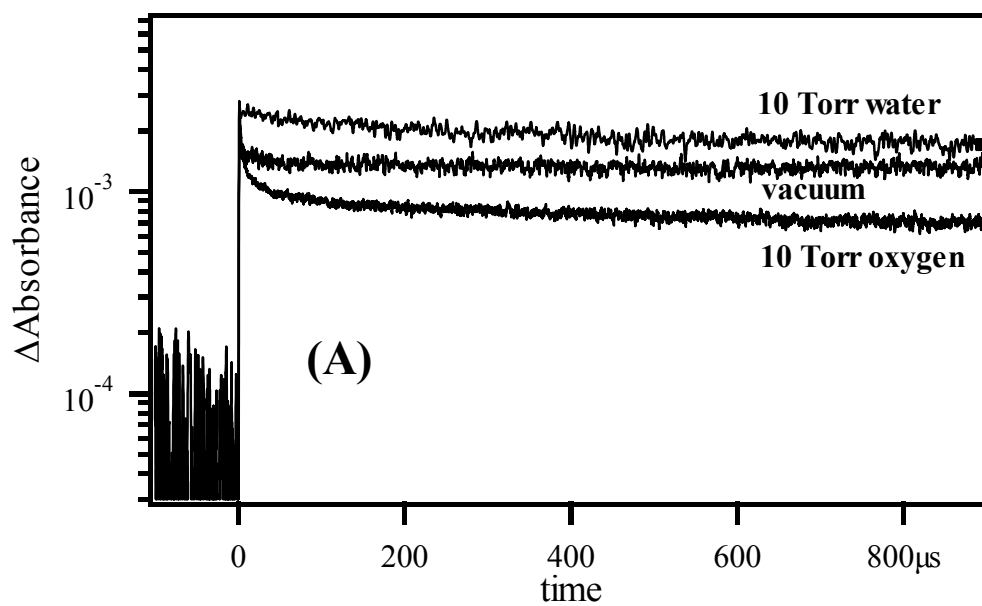**Figure 3**                                                                                          **Takeshita et al.**

**(A)**

600 nm

15.0kV X50.0K 600nm



**(B)**

600 nm

15.0kV X50.0K 600nm

**Figure 4**                                                    **Takeshita et al.**

**Figure 5**                                        **Takeshita et al.**

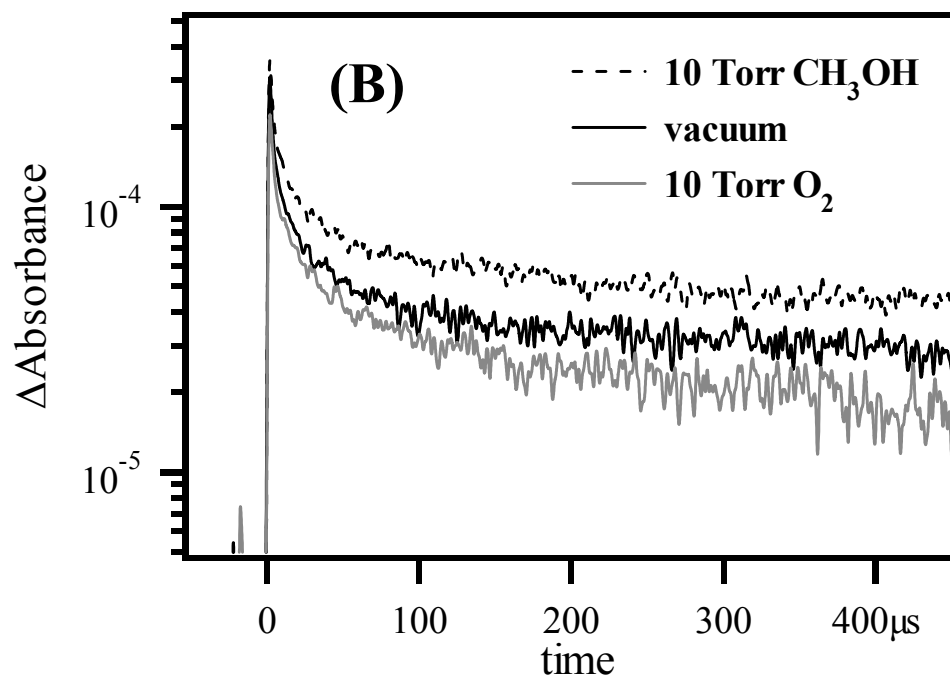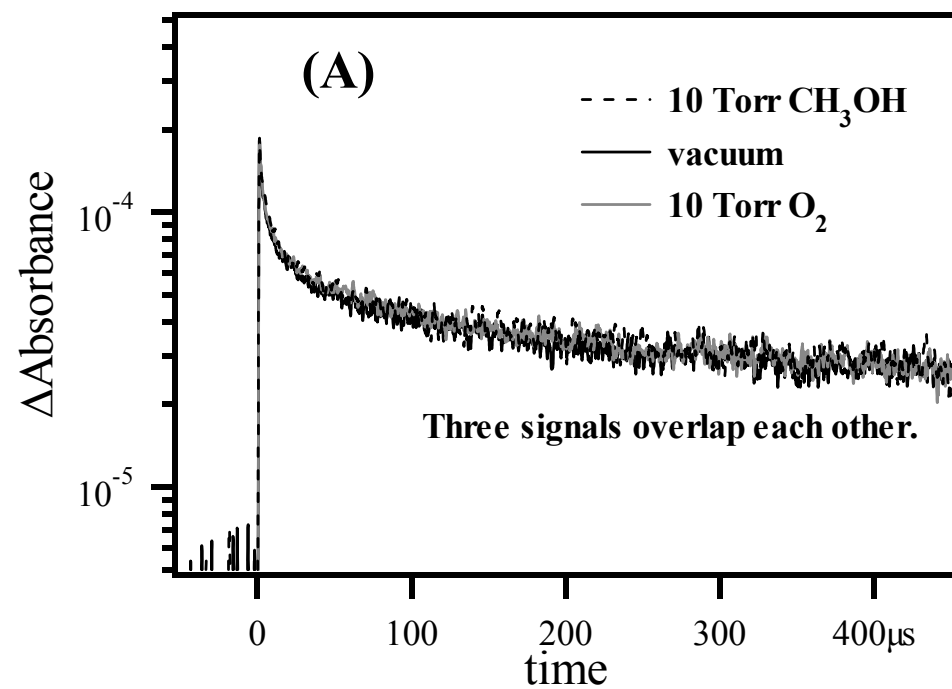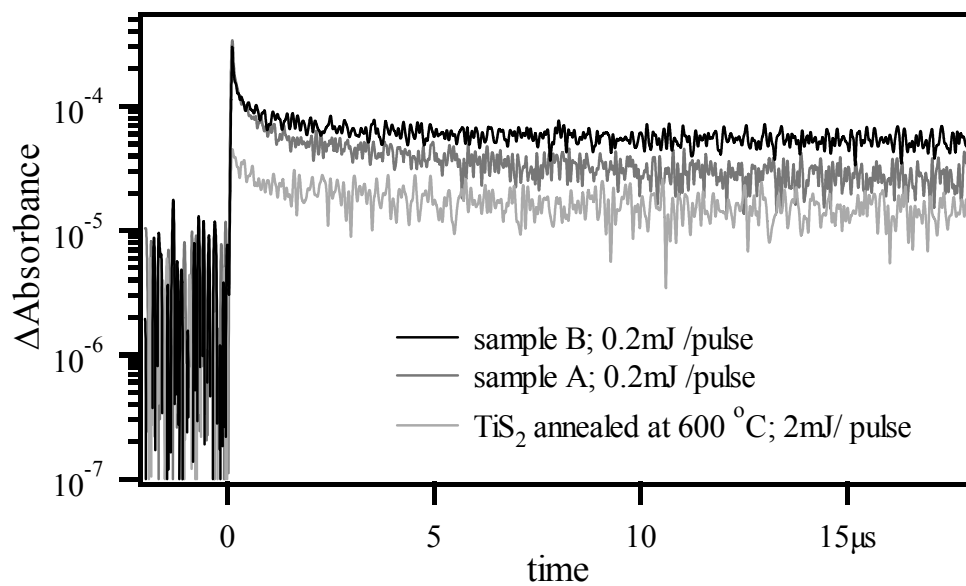**Figure 6**                                                    **Takeshita et al.**

**Figure 8**                                                            **Takeshita et al.**

Energy level

vs NHE / eV

**Figure 9**                                                    **Takeshita et al.**

# A                    # B

1 ~ 2 μm            **Tens of nanometers**